IIETA International Information and Engineering Technology Association
Advancing the World of Information and Engineering

Revue des Composites et des Matériaux Avancés-Journal of Composite and Advanced Materials
Vol. 36, No. 2, April, 2026, pp. 271-280
Journal homepage: http://iieta.org/journals/rcma

Compaction Method Effects on the Mechanical Properties of High-Strength Concrete Incorporating Waste Glass Powder as a Sustainable Substitute

Erwin Sutandar*, Gatot Setya Budi, Ashraf Dhowian Parabi

Department of Civil Engineering, Faculty of Engineering, Tanjungpura University, Pontianak 78124, Indonesia

Corresponding Author Email: erwinsutandar@civil.untan.ac.id

https://doi.org/10.18280/rcma.360205

Received: 20 December 2025
Revised: 6 March 2026
Accepted: 13 March 2026
Available online: 30 April 2026

Keywords:
high-strength concrete, waste glass powder, compaction methods, sustainable construction, compressive strength

ABSTRACT

This study examines the physical and mechanical properties of high-strength concrete (HSC) incorporating 10% refuse glass powder as a partial cement replacement, and assesses the impact of compaction methods. The following three compaction techniques were assessed: manual rodding (V1), internal vibration (V2), and oscillating table (V3). According to SNI 2847:2019, the properties of fresh and hardened concrete were evaluated at 7, 14, and 28 days through slump testing, unit weight determination, and compressive strength measurements. Manual rodding attained superior performance, as evidenced by a 28-day compressive strength of 51.354 MPa. This represents 8.7% and 16.5% improvements over internal vibration (47.237 MPa) and the vibrating table (44.097 MPa), respectively. Unit weight measurements confirmed these findings, with manual rodding achieving the highest density of 2,482.817 kg/m³, compared with 2,472.207 kg/m³ and 2,461.596 kg/m³ for the internal vibration and vibrating table methods, respectively. Manual rodding's superior performance results from the uniform distribution of waste glass powder (WGP) and the optimal particle packing density, which facilitates efficient pozzolanic reactions and the densification of the interfacial transition zone (ITZ). On the other hand, particle segregation was induced by sustained vibrating table operation as a result of the differential settling rates between denser constituents and refuse glass powder. In waste-derived pozzolanic HSC systems, the efficacy is substantially influenced by compaction methodology, as these findings demonstrate.

1. INTRODUCTION

The global construction industry is under increasing pressure to balance environmental sustainability with the growing demand for infrastructure [1]. Concrete manufacturing, which accounts for approximately 8% of global CO_2 emissions, requires innovative strategies to reduce its environmental impact while preserving structural integrity. [2]. The accumulation of non-biodegradable detritus, particularly glass, poses a dual dilemma: resource depletion and environmental degradation [3]. Indonesia's Ministry of Environment and Forestry recorded 291,225.04 kg of unrestrained glass garbage in 2023, highlighting the urgent need for sustainable waste management techniques in the building industry [4]. Waste glass powder (WGP), characterized by its pozzolanic properties and elevated silica content (61.72%), is a viable partial substitute for cement. This approach effectively addresses waste management issues and enhances the sustainability of concrete [5].

Concrete with a compressive strength exceeding 41.4 MPa, also known as high-strength concrete (HSC), has become increasingly important in modern construction projects that require enhanced structural performance and reduced structural dimensions [6]. In HSC compositions, the use of additional cementitious materials, such as refuse glass powder, can improve mechanical properties while reducing reliance on Portland cement [7]. However, the efficacy of WGP in concrete systems is the subject of currently available research, which yields conflicting results [8]. There are studies suggesting a 10–15% increase in strength at replacement levels due to pozzolanic reactions that produce additional calcium silicate hydrate (C-S-H) gel. However, others express apprehensions about the potential for strength reduction and alkali-silica reaction (ASR), particularly when particle fineness and mixture proportions are not tightly controlled [9]. Notably, around 70% of published research concentrates on normal-strength concrete applications, with few systematic studies exploring the behavior of WGP in high-strength systems, where microstructural densification requirements and reduced water-cement ratios pose significantly different consolidation challenges [10].

In addition, the efficacy of the WGP is influenced by factors beyond ordinary substitution ratios, as evidenced by conflicting findings on optimal replacement levels, which range from 10% to 50% across multiple studies [11].

The mechanical properties of concrete are greatly affected

by compaction techniques, which directly impact density, void content, and the quality of interfacial bonding in the hardened matrix [12]. Efficient compaction eliminates entrapped air, which typically accounts for 5–20% of the new concrete volume. This process enhances the binding strength between the cement paste and aggregates and enhances the consolidation of aggregate particles [13]. According to the properties of the concrete mixture and its rheology, a variety of compaction techniques, including manual rodding, internal vibration, and vibratory table methods, offer distinct advantages [14]. Historically, mechanical vibration methods have been regarded as superior to human procedures for attaining maximal density and compressive strength in traditional concrete [15]. Recent preliminary findings indicate unexpected outcomes when utilizing conventional compaction methods on HSC mixtures with fine pozzolanic materials: manual rodding yielded greater compressive strength than vibrating table compaction in WGP-modified HSC, challenging established practices [16]. This paradoxical observation indicates that the interplay between WGP particle attributes (angular morphology, non-absorptive surface, fine particle size distribution) and compaction energy input may modify fresh concrete rheology and consolidation behavior in ways that are not sufficiently comprehended or recorded in existing literature [17].

Despite extensive independent research on the applications of refuse glass powder and compaction techniques, there is a substantial lack of information on the synergistic effects of these factors on the performance of HSC [18]. The impact of incorporating WGP at a 10% replacement level, alongside different compaction energy inputs, on the workability, unit weight, and compressive strength development of HSC systems is not yet clearly defined [19]. This disparity holds significant importance due to: (1) WGP particles exhibiting distinctly different physical properties compared to cement, such as zero water absorption, a smooth surface texture, and angular morphology, which may require modified consolidation methods [20]; (2) HSC composites consisting of low water-cement ratios and superplasticizers produce distinctive rheological conditions that may respond differently to compaction energy than normal-strength concrete [21]; and (3) inadequate or excessive compaction may hinder the optimal efficacy of the pozzolanic reaction and the packaging of particles by altering the vacuum distribution, hemorrhage characteristics, and particle segregation patterns within the matrix [22].

The lack of systematic studies comparing various compaction methods under controlled settings is a significant restriction in contemporary sustainable concrete research [23]. Current research often uses a singular compaction approach, neglecting to assess if other strategies may improve performance for WGP-modified mixes [24]. The mechanistic link between compaction-induced microstructural alterations and the resultant compressive strength in WGP-HSC systems is insufficiently defined, hindering the evidence-based selection of suitable field consolidation methods [25]. This study systematically examines the impact of three distinct compaction techniques—manual rodding (V1), internal vibration (V2), and vibrating table (V3)—on the fresh and hardened characteristics of HSC containing 10% WGP as a partial substitute for cement. The research analyzes essential performance metrics such as workability (slump test), unit weight, and compressive strength at 7, 14, and 28 days, according to SNI 2847:2019 criteria. This research elucidates the correlation between the performance of WGP-modified HSC and compaction techniques, thereby enhancing sustainable construction practices and providing empirical guidance for optimizing structural efficacy and environmental benefits in practical applications. The findings will furnish practitioners with information regarding the most appropriate consolidation methods for waste-derived pozzolanic concrete. They will assess the validity of conventional compaction assumptions in high-performance systems incorporating non-traditional supplementary cementitious materials.

2. MATERIALS

2.1 Cement

Portland Composite Cement (PCC) Type II, manufactured by PT. Conch Cement Indonesia was the primary binding material employed in this investigation. Compatibility with locally procured building materials was ensured by the cement's compliance with the Indonesian National Standard SNI 15-7064-2004 for composite cement and with ASTM C188. The Materials and Construction Laboratory at Tanjungpura University employed the Le Châtelier flask technique to determine a specific gravity of 3.026. The bulk density was measured at 1,260.196 kg/m³ under compacted conditions, and refinement testing revealed that 88% of particles passed through sieve No. 200 (75 μm), suggesting that the grinding was sufficient to facilitate optimal hydration kinetics. While a detailed chemical composition analysis using X-ray fluorescence (XRF) was not conducted for this particular cement batch, the manufacturer's technical data sheets suggest that the typical oxide composition for Indonesian PCC Type II consists of approximately 60–65% CaO, 18–22% SiO_2, 4–6% Al_2O_3, 2–4% Fe_2O_3, 1–3% MgO, and residual alkaline oxides ($Na_2O + K_2O$) below 0.6%. The Blaine specific surface area generally falls between 3,200 and 3,800 cm²/g for this cement grade, facilitating sufficient early-age strength development while ensuring controllable heat of hydration for mass concrete applications. Before concrete mixing, all cement volumes were stored in sealed, moisture-proof containers within a climate-controlled laboratory maintained at 27 ± 2 °C and a relative humidity below 60% to prevent premature hydration reactions.

2.2 Fine aggregate

Natural river sand, categorized as medium-graded aggregate under SNI 7656-2012 Zone III gradation specifications, functioned as the fine aggregate component [25]. Thorough physical property characterization determined an oven-dry specific gravity of 2.582, a saturated surface-dry (SSD) specific gravity of 2.619, and an apparent specific gravity of 2.677, using pycnometer testing methods as specified in SNI 03-1970-1990. The water absorption capacity was measured at 1.431%, indicating a fairly porous internal structure characteristic of naturally river-deposited sands. The analysis of particle size distribution via mechanical sieving confirmed adherence to medium sand classification, resulting in a fineness modulus of 2.51 with a gradual distribution across sieve sizes: 100% passing 4.75 mm, 93% passing 2.36 mm, 68% passing 1.18 mm, 42% passing 0.60 mm, 18% passing 0.30 mm, and 5% passing 0.15 mm. The observed compacted bulk density was 1,527.5 kg/m³, indicating suitable particle

packing properties for HSC applications. The organic impurity concentration assessed by colorimetric testing in accordance with ASTM C40 demonstrated negligible organic contamination (Standard Color No. 1), hence confirming compatibility with cement hydration processes. The clay and silt content passing filter No. 200 (75 μm) was measured at 3.2%, far below the 5% maximum limit established in SNI 03-2847-2019, thereby reducing unnecessary water requirements and ensuring sufficient paste-aggregate interfacial bonding quality. All fine aggregate batches were pre-washed to eliminate surface dust, air-dried to a SSD state, and kept under regulated moisture conditions before batching to guarantee uniform moisture correction during mix proportioning.

2.3 Coarse aggregate

Coarse aggregate consisting of mechanically crushed stone was used, according to ASTM C33-03 gradation designation No. 57, with a nominal maximum aggregate size of 25 mm. The choice of 25 mm NMAS conforms to SNI 03-6468-2000 guidelines for HSC mixes, ensuring an appropriate equilibrium between particle packing efficiency and workability attributes. Physical testing determined an oven-dry specific gravity of 2.669, a SSD specific gravity of 2.684, and an apparent specific gravity of 2.709 in accordance with ASTM C127 standards, while water absorption was recorded at 0.575%, indicating low porosity typical of thick crystalline rock sources. The compacted bulk density of 1,429.125 kg/m³ indicates angular particle shape due to mechanical crushing, which enhances aggregate interlock in the hardened concrete matrix. The mechanical durability evaluated by Los Angeles abrasion testing (ASTM C131) produced a wear coefficient of 23.7% after 500 spins with a specified steel charge, indicating sufficient resistance to mechanical deterioration throughout mixing, handling, and service life. Particle gradation analysis verified adherence to ASTM C33 No. 57 size distribution criteria: 100% passing the 37.5 mm sieve, 95–100% passing the 25.0 mm sieve, 25–60% passing the 12.5mm sieve, 0–10% passing the 4.75 mm sieve, and 0–5% passing the 2.36 mm sieve. The clay and silt concentration was tested at 0.8%, far less than the 1.0% maximum threshold for coarse particles in structural concrete. Before concrete production, all coarse aggregate was meticulously cleansed to eradicate adhering particulates and surface dust, and stored under cover to maintain a consistent moisture content. The aggregate was sourced from approved quarries in the Pontianak area.

2.4 Waste glass powder

WGP was subjected to multi-stage comminution to achieve pozzolanic particle refinement, derived from post-consumer clear soda-lime glass bottles. The source material consisted primarily of discarded beverage bottles collected from local waste management facilities. This material is indicative of the standard municipal glass refuse streams in the Pontianak area. The procedure began with mechanical pulverizing using a laboratory jaw crusher to reduce the particle size to approximately 10–20 mm fragments. Subsequently, the particles were ground in a Los Angeles abrasion machine (ball-mill configuration) for an extended period to produce an ultra-fine powder. The finished product was filtered using U.S. Standard sieve No. 200 (75 μm aperture) to guarantee complete passage, resulting in a fine powder with a particle size distribution akin to standard Type II Portland cement. The prepared waste glass powder used in this research is shown in Figure 1. The physical characterisation determined a specific gravity of 2.490 and a loose bulk density of 1,126.8 kg/m³. While direct measurements of Blaine fineness or BET specific surface area were not performed in this study due to equipment constraints, the sieve No. 200 passage criterion indicates an estimated specific surface area of 3,000–4,000 cm²/g, derived from comparative literature values for similarly processed WGPs. Data on the chemical composition from prior studies of Indonesian waste glass sources reveal a typical oxide level of 61.72% SiO_2, 1.70% Al_2O_3, 0.52% Fe_2O_3, 9.21% CaO, 4.85% MgO, 13.12% Na_2O, along with tiny quantities of K_2O and other trace oxides. This amorphous silica-rich material, distinguished by the lack of crystalline quartz peaks in X-ray diffraction patterns, facilitates pozzolanic reactivity, as the glassy silica interacts with calcium hydroxide released during Portland cement hydration to produce supplementary C-S-H gel phases.

The high alkali content ($Na_2O + K_2O \approx 13–14\%$) raises potential issues related to ASR; however, the ultra-fine particle size below 75 μm significantly reduces expansion risks by facilitating the swift pozzolanic consumption of reactive silica prior to the formation of harmful gel. The WGP was integrated at a constant replacement ratio of 10% by mass of the total cementitious material (cement + WGP), chosen based on literature consensus that suggests optimal enhancement of mechanical performance within the 10–15% substitution range, while ensuring sufficient workability and reducing long-term durability concerns.

Figure 1. Waste glass powder

2.5 Mixing water

The municipal water distribution authority (PDAM–Perusahaan Daerah Air Minum) of Pontianak City supplied potable water for the blending of all concrete volumes. The water supply complied with Indonesian drinking water quality regulations (Permenkes No. 492/2010), ensuring that no harmful contaminants were present that could cause steel reinforcement to corrode or disrupt cement hydration in structural applications. Quality examination confirmed that the pH values were between 6.0 and 7.0, the chloride ion concentration was under 500 ppm, the sulfate content was below 300 ppm, and there was minimal organic matter. Consequently, the water complied with the acceptability standards specified in SNI 03-2847-2019 for mixing concrete. The water-to-cementitious materials ratio (w/cm) was set at 0.406, determined by summing the masses of Portland cement and WGP. This was done to guarantee that the paste volume and hydration kinetics were consistent.

The low water-to-cement ratio, typical of HSC mixes, required the use of chemical admixtures to provide sufficient

workability while maintaining the thick paste microstructure essential for achieving a goal compressive strength greater than 42 MPa. All mixing water was maintained at ambient laboratory temperature (23 ± 2 ℃) before batching to reduce thermal gradients during concrete mixing, which might influence setting properties and early-age strength development.

2.6 Chemical admixture (Superplasticizer)

A polycarboxylate-ether-based high-range water-reducing admixture (HRWRA), commercially designated "SikaCim concrete" and manufactured by PT. Sika Indonesia was employed to enhance workability without increasing the water content, as shown in Figure 2. The admixture conforms to ASTM C494 Type F (high-range water reducer) and Type G (combined high-range water reducer and retarder) classifications, enabling water reduction of 20–30% while maintaining equivalent slump characteristics to reference mixtures. The liquid admixture exhibits a specific gravity of approximately 1.08 ± 0.02, a pH of 6.0 ± 1.0, and a chloride ion content below 0.1%, ensuring compatibility with reinforced concrete applications where corrosion protection is paramount. The dosage rate was fixed at 0.8% by mass of total cementitious materials (cement + WGP), equivalent to approximately 3.8 kg per cubic meter of concrete based on the mixture proportions employed in this study. This dosage was established through preliminary trial batches conducted prior to the formal experimental program, targeting initial slump values of 25–50 mm after mixing without superplasticizer, followed by adjustment to a final slump range of 120–180 mm upon superplasticizer addition immediately before casting operations. The molecular structure of the polycarboxylate-ether functions through electrosteric repulsion mechanisms. This involves the adsorption of negatively charged polymer chains onto positively charged cement particle surfaces, generating strong electrostatic and steric repulsion forces that overcome the attractive van der Waals forces responsible for particle flocculation. This dispersion mechanism ensures that cement particles remain suspended in aqueous media, thereby releasing entrapped water to improve fluidity. It also maintains the mixture's cohesiveness and minimizes segregation tendencies typical of low water-cement ratio mixtures containing fine pozzolanic materials. To ensure uniform distribution throughout the batch, the superplasticizer was promptly added to the combined water shortly before concrete production commenced. The mixture was then vigorously agitated.

Figure 2. SikaCim concrete admixture used in the concrete mixture

2.7 Mixture proportioning

The concrete mixture design followed the procedural methodology outlined in SNI 03-6468-2000 (Pd T-18-1999-03) for HSC formulations. The target characteristic compressive strength (f'c) was specified as 42 MPa at 28 days, representing the lower threshold for HSC classification according to ACI 363R guidelines. Applying a standard deviation of 8 MPa, typical for laboratory-controlled conditions with consistent material quality and a confidence factor of 1.64 for 5% probability of falling below the specified strength, the required mean compressive strength (f'cr) was calculated as 57.4 MPa. It should be noted that f'c and f'cr represent two distinct quantities in mix design methodology: f'c denotes the specified characteristic compressive strength required for structural design purposes, whereas f'cr denotes the required mean compressive strength that must be achieved during laboratory mix design to statistically ensure that f'c is reliably met in practice, accounting for inherent variability in concrete production. The mixture proportions per cubic meter of concrete were established as: 430 kg PCC, 48 kg WGP (10% replacement by mass of total cementitious), 603 kg oven-dry fine aggregate, 1,072 kg oven-dry coarse aggregate, 194 kg water (w/cm ratio = 0.406), and 3.8 kg polycarboxylate superplasticizer (0.8% by mass of cementitious). The aggregate proportions were optimized following the combined aggregate grading approach to achieve maximum packing density, with a coarse-to-fine aggregate ratio of approximately 1.78:1 by mass. All constituent materials were batched by mass using calibrated electronic scales with an accuracy of ±0.1% to ensure reproducibility across the experimental program. Moisture correction factors were applied to aggregate quantities based on pre-determined moisture content measurements conducted immediately prior to each mixing session, with corresponding adjustments to added water quantities to maintain a constant effective w/cm ratio across all batches.

3. METHODS

3.1 Experimental design

This experimental investigation employed a single-factor design with three treatment levels corresponding to distinct compaction methodologies: manual rodding (V1), internal vibration using a mechanical vibrator (V2), and external vibration via vibrating table (V3). The experimental research flowchart is presented in Figure 3. All specimens within each compaction group utilized identical mixture proportions incorporating 10% WGP as partial cement replacement, thereby isolating compaction methodology as the sole independent variable. The experimental program produced a total of 45 cylindrical specimens distributed across two-dimensional configurations: 27 specimens of Ø150 mm × 300 mm for compressive strength testing at 7, 14, and 28-day intervals (three replicates per treatment per age), and 18 specimens of Ø100 mm × 200 mm for unit weight determination and supplementary testing. This sample size distribution provided statistical validity through triplicate measurements while enabling assessment of strength development kinetics across multiple curing ages. All experimental procedures were conducted at the Materials and Construction Laboratory, Department of Civil Engineering,

Tanjungpura University, Pontianak, maintaining consistent environmental conditions (ambient temperature 27 ± 2°C, relative humidity 60–75%) throughout the investigation period from September 2024 to July 2025.

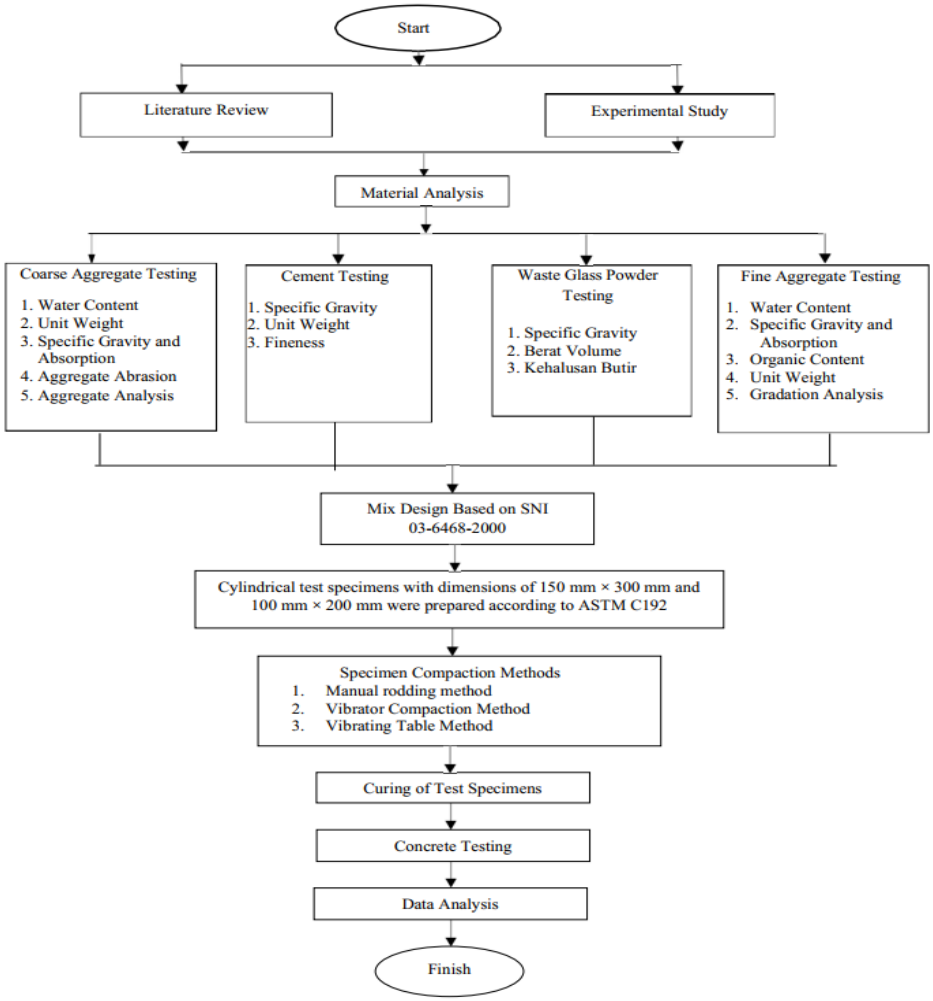

Figure 3. Research flowchart

3.2 Mixing procedure

Concrete batching and mixing operations followed a standardized protocol designed to ensure compositional homogeneity across all specimens. All constituent materials were proportioned by mass using calibrated electronic scales with ±0.1% accuracy, with aggregate moisture corrections applied based on measurements conducted immediately prior to each mixing session. The concrete was prepared using a 400-liter capacity rotary drum mixer operating at approximately 20 revolutions per minute. The batching sequence commenced with the introduction of coarse aggregate, followed by fine aggregate, WGP, and Portland cement, which were dry-mixed for 2 minutes to achieve uniform distribution of solid constituents. Subsequently, mixing water pre-blended with polycarboxylate superplasticizer (SikaCim concrete at 0.8% by cementitious mass) was gradually added while mixing continued for an additional 3 minutes. This wet mixing duration was established through preliminary trials to ensure complete hydration of cementitious particles and thorough dispersion of the superplasticizer without inducing segregation or excessive air entrainment. Following completion of the mixing cycle, a portion of the fresh concrete was extracted for slump testing in accordance with SNI 1972-2008 procedures to verify workability compliance with target range specifications of 120–180 mm after superplasticizer activation.

3.3 Compaction methods

3.3.1 Manual rodding (V1)

Fresh concrete was placed into cylindrical molds in three approximately equal layers, with each layer subjected to 25 uniformly distributed penetrations using a standard steel tamping rod (diameter 16 mm, length 600 mm, hemispherical tip) in accordance with SNI 4810-2013 specifications. The tamping rod penetrated the full depth of each layer, with penetrations extending slightly into the underlying layer to promote interlayer bonding and eliminate horizontal planes of weakness. Following compaction of the uppermost layer, excess concrete was struck off flush with the mold rim using a straight edge, and the external mold surface was tapped lightly with a rubber mallet (10–15 strokes) to release entrapped air bubbles along the mold-concrete interface.

3.3.2 Internal vibration (V2)

Cylindrical molds were filled with fresh concrete in a single continuous pour. A needle vibrator with a 25 mm diameter head operating at approximately 12,000 vibrations per minute was immediately inserted vertically into the concrete mass,

penetrating to within 10 mm of the mold bottom. The vibrator was maintained in position for a duration determined by concrete slump characteristics: 5 seconds maximum for a slump exceeding 75 mm, or 10 seconds maximum for lower slump values, consistent with SNI 03-3976-1995 guidelines. Visual observation of surface gloss development, cessation of large air bubble release, and slight subsidence of the concrete surface served as operational indicators of adequate consolidation. Upon achieving these criteria, the vibrator was slowly withdrawn at a rate not exceeding 75 mm per second to prevent void formation along the extraction path. Supplementary concrete was added if vibration-induced settlement created a surface deficiency, and the specimen surface was finished flush with the mold rim.

3.3.3 Vibrating table (V3)

Fresh concrete was placed into cylindrical molds in a single operation without mechanical compaction, filling to approximately 10 mm above the mold rim to accommodate consolidation-induced settlement. The filled molds were immediately transferred to a vibrating table operating at 3,000–3,600 vibrations per minute with an amplitude of 0.5 mm. Vibration duration was established at 12 seconds based on preliminary optimization [26], representing the minimum duration required to achieve surface gloss development and air bubble cessation without inducing segregation in the low water-cement ratio mixture. Following cessation of vibration, any surface voids were filled with fresh concrete, and the surface was struck off level with the mold rim.

3.4 Curing regime

Following demolding 24 hours after casting, all cylindrical specimens were transferred to a water curing tank maintained at 23 ± 2 °C in accordance with ASTM C192 standard practice for making and curing concrete test specimens in the laboratory. The curing tank contained lime-saturated water (calcium hydroxide concentration approximately 1.5 g/L) to prevent leaching of calcium compounds from the concrete specimens and maintain an alkaline environment conducive to hydration progression. Specimens remained continuously submerged with a minimum 25 mm water coverage above the uppermost surface throughout the designated curing period, with water temperature monitored daily using calibrated thermometers. Water level was replenished as necessary to compensate for evaporation losses, and complete water replacement occurred weekly to maintain clarity and prevent accumulation of dissolved substances. This moist curing protocol ensured consistent hydration conditions across all treatment groups, eliminating moisture availability as a confounding variable in performance comparisons. At the conclusion of each designated testing age (7, 14, or 28 days calculated from the time of initial water-cement contact), specimens were removed from the curing tank, surface-dried with absorbent toweling to achieve a SSD condition, and immediately subjected to the prescribed testing protocol within 30 minutes of removal to minimize moisture content variability.

3.5 Concrete testing

3.5.1 Slump test

Conducted in accordance with SNI 1972-2008 specifications, the standard collapse cone method was employed to evaluate workability. The baseline concrete consistency (target range: 25–50 mm) was established by obtaining initial slump measurements immediately after completion of the dry mixing cycle, but before the addition of superplasticizer. The target workability range (120–180 mm) was verified through final slump testing conducted after the incorporation of superplasticizer and the subsequent 3-minute moist mixing. This range is essential for the efficient consolidation of materials across all compaction methodologies. Three equal layers of the slump cone (top diameter 100 mm, base diameter 200 mm, height 300 mm) were filled, with each layer being subjected to 25 rodding strokes using the standard tamping rod. At the conclusion of the filling and rodding processes, the cone was raised vertically at a consistent rate, and the slump value was determined by the vertical displacement of the concrete mass from its original 300 mm height to the nearest 5mm.

3.5.2 Unit weight determination

Unit weight measurements were conducted on Ø100mm × 200 mm cylindrical specimens at each designated testing age using procedures consistent with ASTM C138. Specimens in SSD condition were weighed using a calibrated electronic balance with 1 gram resolution. Unit weight was calculated as the ratio of specimen mass to geometric volume (computed from measured diameter and height using precision calipers with 0.01 mm resolution), expressed in kg/m³. Three replicate measurements per treatment per age provided statistical reliability and enabled detection of density variations attributable to compaction methodology.

3.5.3 Compressive strength testing

Compressive strength was evaluated using Ø150 mm × 300 mm cylindrical specimens tested at 7, 14, and 28 days in accordance with SNI 2847-2019 provisions. Testing was performed using an MBT universal testing machine with 2,000 kN capacity and a load resolution of 5 kN. Before testing, specimen ends were inspected for planarity and perpendicularity; specimens exhibiting surface irregularities exceeding 0.05 mm were capped using sulfur mortar capping compound to ensure uniform load distribution. Specimens were positioned centrally on the lower bearing plate with longitudinal axis aligned vertically, and axial compressive load was applied at a constant stress rate of 0.25 ± 0.05 MPa/s until specimen failure manifested by audible cracking, load plateau, or visible longitudinal splitting. Maximum applied load at failure was recorded to the nearest 5 kN, and compressive strength was calculated by dividing peak load by the original cross-sectional area. Failure mode classification (columnar, cone, cone-and-split, cone-and-shear, or shear) was documented photographically for each specimen to identify potential testing irregularities or specimen defects.

4. RESULTS AND DISCUSSION

4.1 Fresh concrete workability assessment

Slump testing revealed systematic variations in initial concrete consistency across compaction treatment groups prior to superplasticizer addition, with measured values of 25.33 mm (V1), 27.33 mm (V2), and 30.00 mm (V3). All measurements fell within the target specification range of 25–50mm, validating mixture proportioning accuracy and

eliminating workability as a confounding variable in subsequent compaction performance comparisons. Following superplasticizer incorporation at 0.8% dosage, final slump values increased substantially to 190 mm (V1), 200 mm (V2), and 210 mm (V3), as summarized in Table 1, achieving the target range of 120–180 mm necessary for efficient consolidation in HSC applications. The final slump condition after superplasticizer addition is illustrated in Figure 4. The incremental slump progression from V1 to V3 suggests differential rheological responses attributable to subtle variations in mixing-induced air entrainment or paste distribution heterogeneity rather than systematic formulation differences, given that all batches utilized identical constituent proportions. The polycarboxylate superplasticizer effectively disrupted cement particle flocculation through electrostatic repulsion, liberating entrapped water to enhance fluidity while maintaining satisfactory cohesiveness to resist segregation during handling and placement operations. Optimal superplasticizer dosing for V1 is indicated by the final slump values for V2 and V3, which slightly exceed the upper specification limit. However, there is potential to reduce the dosage slightly in mechanically vibrated systems to prevent excessive fluidity, which may compromise the quality of the paste-aggregate interfacial bonding.

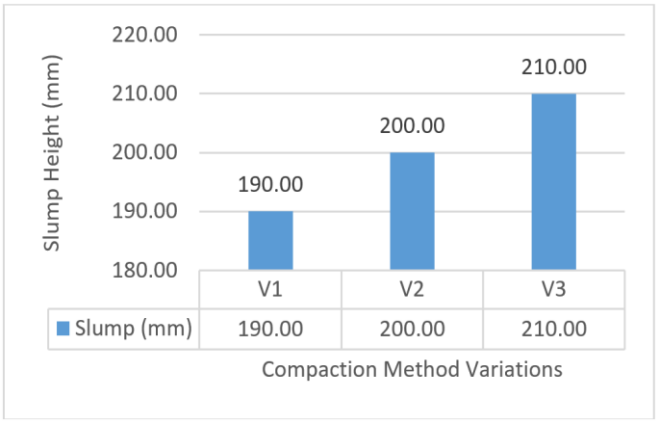

Figure 4. Final slump visualization

Table 1. Slump test

No.	Variation	Slump Height (mm)	Remarks
1	V1	25.33	
2	V2	27.33	Meets Target Slump (25–50 mm)
3	V3	30.00	

4.2 Hardened concrete unit weight analysis

Unit weight measurements at 28-day curing age exhibited systematic density gradients corresponding to compaction methodology, with V1 achieving the highest density of 2,482.817 kg/m³, followed by V2 at 2,472.207 kg/m³, and V3 producing the lowest density of 2,461.596 kg/m³. The average unit weight results at 28 days are summarized in Table 2 and illustrated in Figure 5. This hierarchical density distribution represents relative reductions of 0.427% for V2 and 0.855% for V3 compared to the V1 baseline performance. All three treatment groups satisfied SNI 03-2847-2002 classification criteria for normal-weight concrete (2,200–2,500 kg/m³), confirming adequate consolidation across all compaction methodologies. However, the observed density differentials provide critical mechanistic insights into void structure development and particle packing efficiency. The superior density achieved through V1 indicates that systematic layer-wise compaction with 25 penetrations per layer effectively eliminated large entrapped air voids (typically 3–6 mm diameter) while promoting progressive consolidation through the full specimen depth. This methodical approach ensured penetration into underlying layers, creating interlayer bonding and eliminating horizontal planes of weakness that can develop when successive lifts are inadequately integrated. Conversely, the reduced density in vibrating table specimens (V3) suggests that external vibration applied to the entire formwork assembly may have induced localized segregation phenomena wherein lightweight WGP particles (specific gravity 2.490) migrated toward upper specimen regions due to differential settling rates compared to denser cement particles (specific gravity 3.026) and aggregates (specific gravities 2.490–2.669). This density stratification would create a vertical gradient in paste composition, potentially concentrating weaker, WGP-enriched paste at specimen tops where compressive failure typically initiates during standard testing protocols. The intermediate density of internal vibration specimens (V2) reflects a balance between efficient air void removal through high-frequency oscillation (12,000 vibrations per minute) and minimal segregation risk due to localized vibration zone influence.

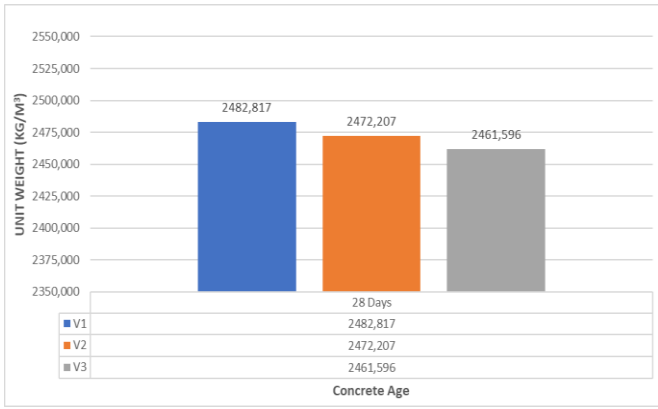

Figure 5. Bar chart of average unit weight

Table 2. Average unit weight

Variation	Unit Weight (kg/m³) 28 Day	Percentage Decrease (%)
V1	2,482.817	0%
V2	2,472.207	0.427%
V3	2,461.596	0.855%

4.3 Compressive strength development kinetics

Throughout the 7 to 28 day curing period, the compressive strength consistently followed a clear ranking. V1 achieved 41.211 MPa at 7 days, 47.407 MPa at 14 days, and 51.354 MPa at 28 days; V2 produced 41.253 MPa, 45.455 MPa, and 47.237 MPa at corresponding ages; while V3 consistently showed the lowest strength, ranging from 38.197 MPa at 7 days to 44.097 MPa at 28 days. The compressive strength test results are summarized in Table 3, while the comparison of compressive strength development among V1, V2, and V3 is presented in Figure 6. All treatment groups substantially exceeded the specified characteristic strength of 42 MPa at 28 days, validating the efficacy of 10% WGP substitution in HSC formulations. The strength ranking contradicts conventional

expectations that mechanical vibration universally enhances concrete compressive performance, necessitating detailed mechanistic examination of the compaction-microstructure-strength relationship chain.

Table 3. High-strength concrete (f'c) compressive strength test results with different compaction methods

Compaction Method	Compressive Strength (MPa)		
	7 Days	14 Days	28 Days
V1 (Manual Rodding)	43.163	49.784	55.513
	42.144	43.927	49.402
	38.325	48.510	49.147
V2 (Internal Vibrator)	41.253	45.455	47.237
	40.489	41.890	58.187
	39.852	40.744	41.635
V3 (Vibrating Table)	37.306	38.706	42.781
	38.834	40.998	46.219
	38.452	40.362	43.290

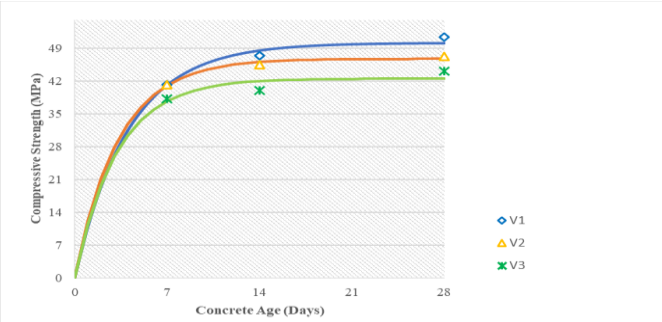

Figure 6. Mean compressive strength of V1, V2, and V3 at 7, 14, and 28 days
Note: Data points represent the average of three replicate specimens; individual specimen values are reported in Table 3

The superior strength performance of V1 at 28 days—representing 8.7% enhancement over V2 and 16.5% enhancement over V3—originates from synergistic effects of optimal particle packing density and minimized microstructural defects. According to Féret's strength-porosity relationship, compressive strength exhibits exponential sensitivity to volumetric air void content, with each 1% increase in porosity reducing strength by approximately 5–7% in high-strength systems. The higher unit weight of V1 specimens (2,482.817 kg/m³) compared to V3 (2,461.596 kg/m³) corresponds to approximately 0.855% density differential, which translates to estimated porosity reduction of 0.5–0.8% based on Powers and Brownyard's gel-space ratio model. This porosity reduction directly enhances load-bearing capacity by increasing the effective cross-sectional area of solid material resisting applied stress and reducing stress concentration sites at void peripheries where crack initiation preferentially occurs. Furthermore, systematic manual rodding promoted uniform distribution of the fine WGP particles (100% passing sieve No. 200, equivalent to < 75 μm) throughout the cement paste matrix, optimizing the spatial distribution of pozzolanic reaction sites. The WGP's reactive amorphous silica (SiO_2 content 61.72%) undergoes secondary hydration reactions with calcium hydroxide liberated from Portland cement hydration according to the pozzolanic equation: $Ca(OH)_2 + SiO_2 + H_2O \rightarrow$ C-S-H gel . This reaction progressively densifies the interfacial transition zone (ITZ) between aggregate particles and bulk cement paste—historically the weakest microstructural region in conventional concrete—through formation of additional C-S-H gel with a lower calcium-to-silica ratio (C/S ≈ 1.2–1.5) compared to primary C-S-H from cement hydration (C/S ≈ 1.7–2.0). The denser, more polymerized C-S-H structure exhibits enhanced mechanical interlocking and reduced nanoporosity, contributing to strength gains beyond those attributable solely to void reduction.

The unexpected underperformance of vibrating table compaction (V3) despite its widespread adoption in precast concrete production facilities illuminates critical limitations when applying this methodology to low water-cement ratio, pozzolan-modified HSC. The combination of elevated paste fluidity induced by superplasticizer addition (final slump 210 mm) and sustained whole-body vibration (3,000-3,600 vibrations per minute for 12 seconds) created conditions conducive to aggregate segregation and paste stratification. During vibration, the concrete mass transitions to a pseudo-liquid state wherein individual aggregate particles experience gravitational settling forces that exceed viscous resistance forces from the surrounding paste. Stokes' Law predicts settling velocity as proportional to the square of particle diameter and directly proportional to the density differential between the particle and suspending medium. Consequently, coarse aggregate particles (maximum size 25 mm, specific gravity 2.669) settled preferentially toward mold bottoms, while fine WGP particles (median size < 37 μm, specific gravity 2.490) exhibited reduced settling rates and accumulated in upper specimen regions. This vertical heterogeneity is characterized by reduced strength, as standard cylindrical compression testing applies a load parallel to the casting direction. This failure to initiate in the weaker, WGP-enriched top region may result in an incomplete pozzolanic reaction at 28 days, as the stoichiometric availability of calcium hydroxide for pozzolanic consumption is exceeded by the locally elevated WGP concentrations. Furthermore, the initial cement hydration period may have been disrupted by the duration of excessive vibration (specimens were vibrated within 30 minutes of water-cement contact), which could have slowed the development of early-age strength despite the adequate consolidation at later ages.

4.4 Comparative analysis with theoretical predictions and previous research

The experimental strength results can be contextualized through comparison with established predictive models and published literature on WGP concrete. According to the Andreasen particle packing model—which optimizes aggregate gradation through power-law distribution functions to maximize packing density—the ideal compaction methodology should minimize void volume while maintaining spatial homogeneity of constituent phases. The manual rodding protocol (V1) approximates this ideal condition through its systematic, layer-by-layer consolidation approach that prevents preferential particle migration while progressively eliminating entrapped air. This finding aligns with theoretical expectations from the Densified Mixture Design Algorithm (DMDA), which prioritizes achieving minimum void content through optimized particle size distribution and appropriate consolidation energy input. The DMDA framework would predict that excessive vibration energy (as potentially occurred in V3) disrupts optimal packing arrangements by allowing particles to reorient into less stable configurations or creating localized regions of

excess paste that contribute minimal strength enhancement.

Comparison with previous investigations reveals both consistencies and notable deviations. Karwur et al. [27] reported an optimal compressive strength of 31.1 MPa at 10% WGP replacement in normal-strength concrete, substantially lower than the 51.354 MPa achieved in this study for V1 specimens. This performance enhancement reflects the synergistic benefits of high-strength mixture design (low w/c ratio of 0.406, superplasticizer incorporation) combined with optimized compaction methodology. However, earlier work by Ardiwinata [28] documented that mechanical vibration produced 124.25% strength achievement at 28 days compared to 117.12% for manual rodding in conventional concrete, a trend opposite to current findings. This discrepancy underscores the critical interaction between mixture rheology (particularly paste viscosity and yield stress modified by superplasticizer and pozzolan addition) and compaction energy input. The cohesive, high-viscosity paste produced in the present study was resistant to segregation under moderate manual compaction due to the low water-cement ratio and fine WGP particles. However, it was susceptible to particle migration under sustained high-amplitude vibration. This observation implies that the optimization of compaction methodology must take into consideration the specific characteristics of the mixture, rather than incorporating universal protocols across a variety of concrete formulations.

4.5 Strength development trajectory and maturity considerations

Examination of strength gain rates between testing ages provides insights into hydration kinetics and pozzolanic reaction progression. The V1 specimens exhibited strength increases of 14.9% between 7–14 days and 8.3% between 14–28 days, indicating continued hydration and pozzolanic activity beyond the primary strength development period. This extended strength gain contrasts with conventional Portland cement concrete, which typically achieves 70–75% of 28-day strength by 7 days and exhibits minimal gains after 14 days. The persistent strength enhancement in WGP-modified concrete reflects the slower kinetics of pozzolanic reactions compared to primary cement hydration, as the pozzolanic process depends on diffusion of calcium hydroxide from cement hydration sites to WGP particle surfaces—a transport-limited mechanism requiring extended time periods. According to comparable strength trajectories across all compaction methods, the pozzolanic reaction kinetics were relatively unaffected by the consolidation method. This suggests that the strength differences are primarily due to variations in void content rather than differences in the extent of the chemical reaction. Nevertheless, the absolute strength values at each age consistently indicated that manual rodding was the preferred method, thereby confirming that the microstructural quality established during initial consolidation remains intact throughout the curing period and cannot be remedied solely by continued hydration. This discovery underscores the critical importance of appropriate initial compaction for achieving target performance in HSC systems modified with pozzolan.

5. CONCLUSIONS

This experimental investigation systematically evaluated the influence of three distinct compaction methodologies—manual rodding (V1), internal vibration (V2), and vibrating table (V3)—on the fresh and hardened properties of HSC incorporating 10% WGP as partial cement replacement. Compressive strength testing at 28-day curing age demonstrated that manual rodding achieved a superior performance of 51.354 MPa, exceeding the specified characteristic strength of 42 MPa by 22.2%, while internal vibration and vibrating table yielded 47.237 MPa (8.7% reduction) and 44.097 MPa (16.5% reduction), respectively. This strength hierarchy contradicts conventional expectations that mechanical vibration universally enhances concrete performance, revealing critical interactions between low water-cement ratio (0.406), fine pozzolan particle characteristics (100% passing 75 μm sieve), and consolidation energy input. Unit weight measurements corroborated these findings, with manual rodding producing the highest density of 2,482.817 kg/m³ compared to 2,472.207 kg/m³ for internal vibration and 2,461.596 kg/m³ for vibrating table. The mechanistic origins of manual rodding's superiority lie in the optimal particle packing density achieved through systematic layer-wise consolidation. This procedure prevents the preferential migration of lightweight WGP particles (specific gravity 2.490) while eliminating large entrapped air voids. In contrast, sustained vibrating-table operation induces vertical density stratification by differential settling of constituents with disparate specific gravities.

REFERENCES

[1] Murtagh, N., Scott, L., Fan, J. (2020). Sustainable and resilient construction: Current status and future challenges. Journal of Cleaner Production, 268: 122264. https://doi.org/10.1016/j.jclepro.2020.122264

[2] Torres, B.M., Völker, C., Firdous, R. (2023). Concreting a sustainable future: A dataset of alkali-activated concrete and its properties. Data in Brief, 50: 109525. https://doi.org/10.1016/j.dib.2023.109525

[3] Yang, Z., Ji, X., Sha, X.L., Ding, J., Cheng, L., Li, G. (2025). An eco-friendly adhesive with ultra-strong adhesive performance. Polymer Chemistry, 16(8): 954-962. https://doi.org/10.1039/d4py01398k

[4] Augustin, E., Karlinasari, L. (2024). Analysis of MEP work waste management efforts in building construction projects in Jakarta Greater Area. Journal of Natural Resources & Environment Management/Jurnal Pengelolaan Sumberdaya Alam dan Lingkungan, 14(3): 590. https://doi.org/10.29244/jpsl.14.3.590

[5] Sivasuriyan, A., Koda, E. (2025). Incorporation of waste glass powder in the sustainable development of concrete. Materials, 18(14): 3223. https://doi.org/10.3390/ma18143223

[6] Elrefaei, A.E., Alsaadawi, M., Elshafiey, M.M., Abdolwahab, M., Oan, A.F. (2024). Performance evaluation of ultra high performance concrete manufactured with recycled steel fiber. Advances in Science and Technology, 152: 3-13. https://doi.org/10.4028/p-dwhx1h

[7] Benfrid, A., Bouiadjra, M.B. (2024). Investigation of instability in waste glass-based eco-concrete panels under thermomechanical buckling loads. Studies in Engineering and Exact Sciences, 5(2): e6886. https://doi.org/10.54021/seesv5n2-108

[8] Khan, F.A., Shahzada, K., Ullah, Q.S., Fahim, M., Khan, S.W., Badrashi, Y.I. (2020). Development of environment-friendly concrete through partial addition of waste glass powder (WGP) as cement replacement. Civil Engineering Journal, 6(12): 2332-2343. http://dx.doi.org/10.28991/cej-2020-03091620

[9] Mohammadi, A., Ghiasvand, E., Nili, M. (2020). Relation between mechanical properties of concrete and alkali-silica reaction (ASR); a review. Construction and Building Materials, 258: 119567. https://doi.org/10.1016/j.conbuildmat.2020.119567

[10] Gowthaman, S., Sudha, C. (2024). Characteristics strength of high-performance concrete with the interaction of silica fume and GGBS. AIP Conference Proceedings, 3187(1): 020009. https://doi.org/10.1063/5.0236196

[11] Ahmad, J., Zhou, Z., Usanova, K.I., Vatin, N.I., El-Shorbagy, M.A. (2022). A step towards concrete with partial substitution of waste glass (WG) in concrete: A review. Materials, 15(7): 2525. https://doi.org/10.3390/ma15072525

[12] Kanellopoulos, A., Savva, P., Petrou, M.F., Ioannou, I., Pantazopoulou, S. (2020). Assessing the quality of concrete-reinforcement interface in Self Compacting Concrete. Construction and Building Materials, 240: 117933. https://doi.org/10.1016/j.conbuildmat.2019.117933

[13] Meko, B., Ighalo, J.O., Ofuyatan, O.M. (2021). Enhancement of self-compactability of fresh self-compacting concrete: A review. Cleaner Materials, 1: 100019. https://doi.org/10.1016/j.clema.2021.100019

[14] Şengün, E., Alam, B., Shabani, R., Yaman, I.O. (2019). The effects of compaction methods and mix parameters on the properties of roller compacted concrete mixtures. Construction and Building Materials, 228: 116807. https://doi.org/10.1016/j.conbuildmat.2019.116807

[15] Zhang, J., Peng, L., Wen, S., Huang, S. (2024). A review on concrete structural properties and damage evolution monitoring techniques. Sensors, 24(2): 620. https://doi.org/10.3390/s24020620

[16] Nas, M., Akpinar, M.V. (2025). Towards a refined standard for molding roller-compacted concrete (RCC) using vibrating hammers. International Journal of Pavement Research and Technology, 1-27. https://doi.org/10.1007/s42947-025-00676-4

[17] Feys, D., De Schutter, G., Khayat, K.H., Verhoeven, R. (2016). Changes in rheology of self-consolidating concrete induced by pumping. Materials and Structures, 49(11): 4657-4677. https://doi.org/10.1617/s11527-016-0815-7

[18] Chen, G., Suhail, S.A., Bahrami, A., Sufian, M., Azab, M. (2023). Machine learning-based evaluation of parameters of high-strength concrete and raw material interaction at elevated temperatures. Frontiers in Materials, 10: 1187094. https://doi.org/10.3389/fmats.2023.1187094

[19] Tahwia, A.M., Essam, A., Tayeh, B.A., Abd Elrahman, M. (2022). Enhancing sustainability of ultra-high performance concrete utilizing high-volume waste glass powder. Case Studies in Construction Materials, 17: e01648. https://doi.org/10.1016/j.cscm.2022.e01648

[20] Lam, W.L., Cai, Y., Sun, K., Shen, P., Poon, C.S. (2024). Roles of ultra-fine waste glass powder in early hydration of Portland cement: Hydration kinetics, mechanical performance, and microstructure. Construction and Building Materials, 415: 135042. https://doi.org/10.1016/j.conbuildmat.2024.135042

[21] Kovler, K., Roussel, N. (2011). Properties of fresh and hardened concrete. Cement and Concrete Research, 41(7): 775-792. https://doi.org/10.1016/j.cemconres.2011.03.009

[22] Joseph, A., Bala Murugan, S. (2025). Impact of pozzolanic additives on compressive strength and elastic modulus of high-strength self-compacting concrete. Engineering Research Express, 7(3): 035124. https://doi.org/10.1088/2631-8695/adfaca

[23] Al-Neami, M.A., Nsaif, M.H. (2024). Remediation of expansive soils utilizing waste glass powder. IOP Conference Series: Earth and Environmental Science, 1374(1): 012027. https://doi.org/10.1088/1755-1315/1374/1/012027

[24] Mahmoud, A.A., El-Sayed, A.A., Aboraya, A.M., Fathy, I.N., Zygouris, N., Sadollah, A., Agwa, I.S., Tayeh, B.A., Asteris, P.G. (2025). Synergizing machine learning and experimental analysis to predict post-heating compressive strength in waste concrete. Structural Concrete, 26(3): 2916-2950. https://doi.org/10.1002/suco.202400211

[25] Ramdani, Y., Azizah, N., Herlina, N. (2024). The effect of different concrete mix designs and maximum aggregate size variations on the compressive strength of normal concrete. Geomate Journal, 26(118): 87-95.

[26] Suryadi, D., Nurtanto, D., Widayanto, E. (2021). Effect of frequency and duration of vibration on a vibrating table against compressive strength of concrete [in Indonesian]. Jurnal Rekayasa Sipil dan Lingkungan, 5(2): 176-183. https://doi.org/10.19184/jrsl.v5i2.25540

[27] Karwur, H.Y., Tenda, R., Wallah, S.E., Windah, R.S. (2013). Compressive strength of concrete with glass powder as a partial cement substitute [in Indonesian]. Jurnal Sipil Statik, 1(4): 276-281. Available: https://ejournal.unsrat.ac.id/v2/index.php/jss/article/view/1396.

[28] Ardiwinata, Y. (2014). Study on the effect of three fresh concrete compaction methods on the compressive strength and segregation of K-300 concrete (f'c = 24.9 MPa) [in Indonesian]. Jurnal Teknik Sipil dan Lingkungan, 2(3): 407-412. https://garuda.kemdiktisaintek.go.id/documents/detail/475151.